DEVELOPMENT of a PRODUCTION APPROACH to BUILD a TITANIUM FLAPERON RIB by DIRECTED ENERGY DEPOSITION

Maria L. Montero-Sistiaga[1*ORCID], Ralph Haagsma[1], Timo Osinga[1], Unai San Martin Echezarreta[1], Marc de Smit[1], Peter Nijhuis[1]

[1] Royal NLR-Netherlands Aerospace Centre, Marknesse, The Netherlands

* Corresponding Author: maria.montero@nlr.nl

Abstract

Laser Powder Directed Energy Deposition (LP-DED) is gaining interest in the production of complex large parts at a high production rate compared to conventional machining. Typically, these products are milled out of solid blocks. The aim of this work is to show the whole production chain to manufacture a titanium flaperon rib starting from the process optimisation to production and post-processing of the part itself.

First, the process parameters for thin and bulky structures were optimised in LP-DED. Then, different characteristic design features of the rib were defined and the manufacturing strategies were optimised. Lastly, all optimised strategies were applied for the production of the full-scale flaperon ribs.

In this work, several design guidelines and optimum process conditions were obtained for Ti6Al4V processed by LP-LP-DED. On one hand, the process parameters for thin walls and solid features were obtained. In addition, intersections and overhang structures were studied to achieve stable and high-quality connections. On the other hand, different strategies for reducing the deformations were studied and minimum deformations were obtained for large slender build plates. All developed strategies were implemented to successfully produce a large-sized flaperon rib in Ti6Al4V by powder LP-DED.

Keywords: Directed Energy Deposition, design guidelines, process optimisation, titanium, flaperon rib

1 Introduction

Additive Manufacturing (AM) is becoming very attractive for producing functional components. Directed Energy Deposition (DED) is one of the emerging AM processes that is also gaining interest in producing large parts at higher build rates. DED consists of building 3D components by depositing layers onto a substrate or a pre-existing part. The feedstock can be a powder or a wire and the energy source can be a laser beam, plasma or electron beam.

The high design freedom that DED gives makes it an interesting process for producing near-net shape aircraft components. DED can allow the production of more complex rib structures with multi-function component manufacturing within one part. This can lead to weight and cost reductions, by also increasing the functionality and hence the fuel burn-emission and maintenance effort. Moreover, the manufacturing time for complex components can be significantly reduced by DED compared to conventional manufacturing such as casting/forging and milling.

In addition, in the aerospace sector, the buy-to-fly (BTF) ratio is of great importance as a reference for manufacturing efficiency. BTF ratio refers to the relation between the initial weight of the raw material to the final part material. The BTF ratios for subtractive manufacturing in real applications are between 40:1 and 10:1 [1]. In contrast, for AM processes ratios between 1:1 and 3:1 are commonly found in the literature [2], [3].

Titanium alloys are widely used in aircraft components, thanks to their high specific strength. Moreover, titanium components can be combined with high-temperature thermoplastics and do not suffer from galvanic corrosion when joined to carbon fibre parts. However, many times, manufacturing and milling complex components made of titanium alloys can be challenging. Several studies have reported on the manufacturing of titanium parts by DED [4]–[6]. The mechanical performance of DED titanium parts show typically higher tensile strength, but lower ductility, compared to the components produced by conventional methods, such as casting and forging [7].

Besides the advantages that DED of titanium offers, there are still challenges related to DED design limitations. There are already works published on design guidelines

as well as an ASTM DED design guideline [8] which can support design for DED.

In this work, the workflow for producing a titanium flaperon rib is described. First, the process parameter optimisation is described to obtain highly dense and smooth thin structures. Then, the most critical features of the rib were identified and several strategies were developed for efficient production. Lastly, the different stages for manufacturing the flaperon rib are described.

2 Materials and methods

In this work, Ti6Al4V powder from Oerlikon Metco Inc. was used with a particle size distribution of d10 of 52.9 µm, d50 of 70.1 µm and d90 of 109.80 µm. The production of the parts was carried out using a BeAM Modulo 400 DED, 5-axis gantry machine. The building was performed under an argon atmosphere. The used nozzle has a maximum laser power of 2 kW and a spot diameter of 2.2 mm. The machine is also equipped with four vibratory hoppers from Medicoat.

The final design of the flaperon rib is shown in Figure 1. The substrate is shown in black colour and it is located at the centre of the geometry. The substrate is 6 mm thick and it is part of the final flaperon rib. The geometry consists of mostly thin-walled features with intersecting walls. These walls were designed with a thickness of 2.3 mm. On the right hand, highlighted in orange, an asymmetric box structure is built. Perpendicular to this box, an overhanging 8 mm horizontal web is placed. Lastly, an 8 mm thick lug is applied on the side surface of the box. The total dimensions of the flaperon rib are 700 mm in length, 210 mm in width and 300 mm in height.

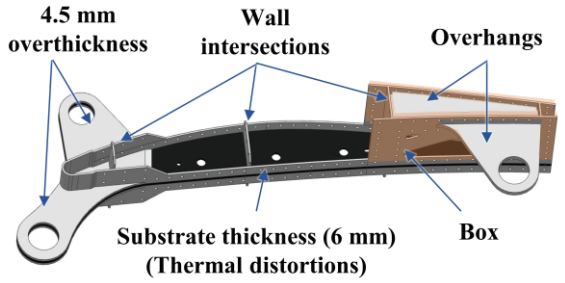

Figure 1: Flaperon rib design with characteristic features.

Before building the final ribs, several process optimisation steps were carried out. First, the parameters of thin walls were optimised by building several thin walls with varying parameters. Next, the offsets of wall intersections were optimised. Then, different features were deposited on top of thin plates in order to evaluate and reduce deformations. Lastly, several strategies were evaluated to weld an 8 mm plate into the box structure.

During the production and optimisation, different substrates were used, all cut out of Ti6Al4V alloy plates. For the process parameter optimisation, 20 mm thick plates were used. Deformation tests were done on thin 5 mm plates only clamped at one side. Lastly, in the flaperon rib, the substrate chosen was 6 mm thick and it was incorporated as part of the structure. In total, three full-scale ribs were manufactured.

In order to evaluate the quality, porosity and microstructure of the parts, the samples were ground and polished using OP-S suspension. For optical micrographs, an Axioplan 2 microscope was used. Kroll's reagent (10 ml H_2O, 2 ml HF and 6 ml HNO_3) for 20 seconds.

The ribs were heat treated twice in a vacuum oven at Bodycote Brazing (The Netherlands). The first time the ribs were heat treated separately and clamped in the fixture in order to avoid deformations of the substrate. Once the DED steps were finalised, the ribs were again treated. The heat cycle was stress relief treatment at 788 °C for two hours.

3 Results and discussion

3.1 Process parameter optimisation

The rib mainly consists of thin-walled features with a thickness of 2.3 mm. For that, first, thin wall parameters needed to be optimised. Thin walls were produced with varying laser power (P) and travel speed (v), 1100-1400 W and 1475-1975 mm/min, respectively. The layer thickness was kept constant at 0.66 mm and the powder feed rate to 15 g/min.

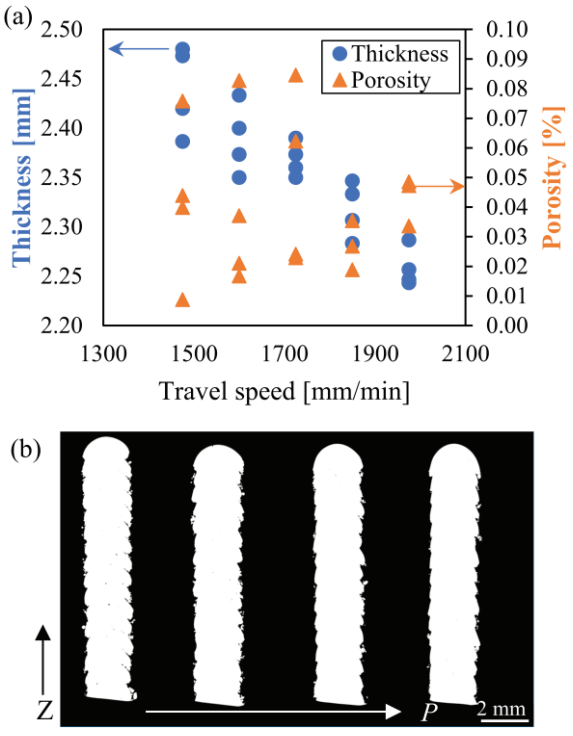

Figure 2: (a) Thickness and porosity evolution with respect to the travel speed and (b) cross-sections of walls produced at 1975 mm/min with increasing laser power.

In Figure 2(a), the thickness and porosity of the built thin walls are shown. It is observed that the wall thickness decreases linearly with increasing travel speed. In contrast, the speed does not have a significant effect on the porosity for the analysed range. The desired thickness (2.3 mm) is obtained with the highest travel speed. In Figure 2(b), the cross-sections of the wall built with 1975 mm/min are shown with increasing laser power. The roughness decreases with increasing laser power, decreasing the bumps between layers.

The design of the flaperon rib also contains intersecting walls as shown in Figure 1. For that, variable offset wall intersections were built to select the best configuration, building a single component as shown in Figure 3. The web length was kept constant and the start position was varied to create an offset variation between 0 to 1.15 mm to the centreline of the flanges. This test allows the evaluation of a large number of offset values within one component. An offset value lower than 0 mm is not recommended since this would lead to too much material deposition at the interface. The 1.15 mm offset was chosen as the maximum, considering the width of around 2.3 mm of a single wall. The quality of the intersection was examined by looking at the cross-sections. It was concluded that the best quality was obtained for offsets lower than 0.2 mm. As shown in Figure 3(b), 0.5 and 1 mm offsets result in porous intersections and necking, which indicates poor interface quality.

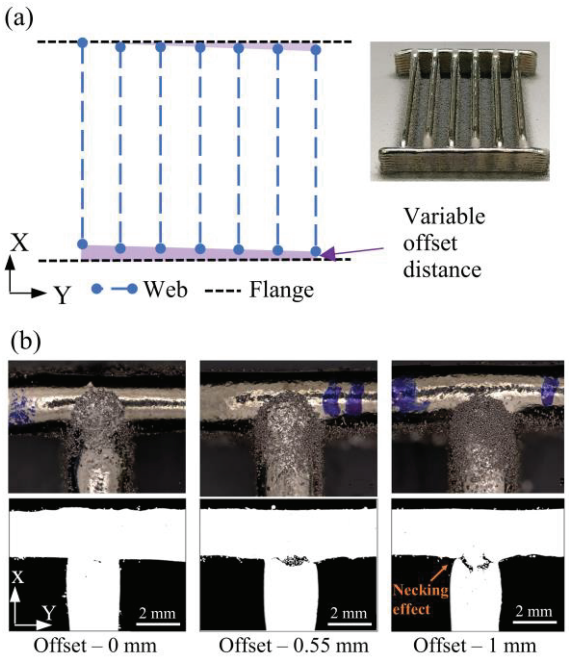

Figure 3: (a) Schematic representation of the intersecting wall geometry and (b) cross-sections of the intersections with an offset of 0, 0.55 and 1 mm.

3.2 Deformation test

Material is added on a substrate plate which has a thickness of 6 mm and a length of around 700 mm. Since the applied heat during DED production can induce deformations, some prior deformation tests were performed on 5 mm thick substrates. During material deposition, the plates were clamped only on the left side.

First, a U-shape geometry was made along the contour in a continuous mode to a total height of 13 mm. After the deposition of each layer, the deformation along the Z-direction was measured. The largest deformation occurred within the first three layers, obtaining a total deformation of 2 mm after depositing 20 layers as shown in Figure 4(a).

Second, a solid block was deposited on the thin plate, alternating the depositing path 0° and 90° along the long axis. The Z deformation was again measured after every layer. The first layer was applied longitudinally (0°) and it resulted in more than 2 mm deformation. The second transverse layer (90°) did not increase the deflection in Z-direction. In total, five layers were deposited and the measured maximum deflection was 6 mm, as shown in Figure 4(b). From this test, it can be concluded that rotating the depositing path helps reduce deformation. In addition, it is preferred to avoid long vectors along the longitudinal direction of the substrate.

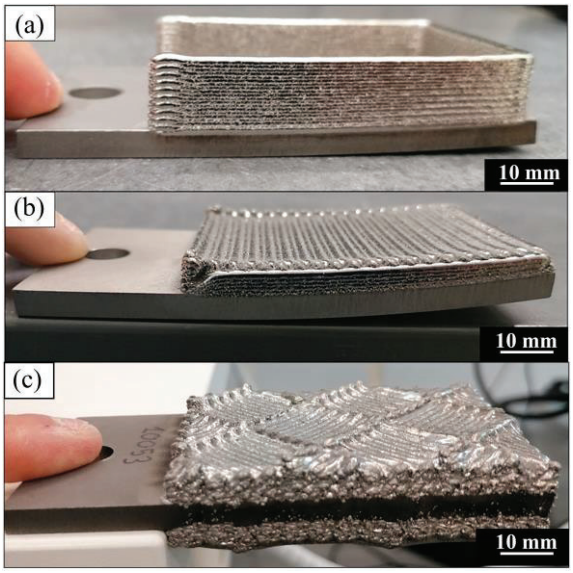

Figure 4: (a) U-shape, (b) solid block with 0-90° strategy and (c) island and symmetric build-up strategy built on 5 mm substrates.

In the last test, the aim was to find a strategy leading to the minimum amount of deformation. Wang et al. [2] showed that islands of approximatively 20-30 mm, deposited from outside to inside, in a zig-zag manner and as randomly as possible, lead to the lowest substrate deformation in DED of Ti6Al4V. Therefore, the same strategy was applied in this third test. Islands of 25x25 mm were built tilted 45° to the longitudinal axis. Each island was deposited in a zig-zag manner and the pattern was rotated 90° between each layer. On top of that, the symmetrical build-up was used to compensate for

deformations. Figure 4(c) shows that deformation-free deposition was obtained when depositing with the island strategy and in a symmetrical build-up manner. After the first deposited layer, a maximum deformation of 1 mm was obtained. The second layer was built on the other side, which lead to full compensation of the initial deformation.

3.3 Overhang features

Overhanging features are challenging in DED at difficult to reach zones or when 5-axis deposition is not possible. In the flaperon rib structure, a horizontal web is designed inside the box (see Figure 1). This plate is 8 mm in thickness. Due to DED limitations to build such a horizontal web, the possibility of welding a plate using DED was evaluated. Since the use of DED to weld plate material was not found in the literature, some tests were done by manufacturing three tubes of 50x50x20 mm and welding plates on top of them. In order to ensure good connection between the DED added material and the plate, 50x50x5 mm plates were machined with varying chamfer inclinations. The schematic representation of the welding test with DED is shown in Figure 5(a). In Figure 5(b), an example of the welding test on the overhanging plate is shown.

In Figure 6, the cross-sections of the welds on top of the three different chamfer inclinations are shown. It can be observed that the pores between the deposited material and the plate are smaller for lower angles. Therefore, it is preferred to have a lower angle chamfer to ensure a good connection with minimum porosity. Looking at the deposited material, a larger height is reached compared to the thickness of the plate, although it was designed to have the same height. Due to the overhanging nature of the feature, the heat cannot be dissipated as good as through a solid substrate which causes an overheating effect. Hence, the melt pool becomes larger in the last deposited layers, as seen in Figure 6(c). Nevertheless, the deposited material shows no significant porosity percentage.

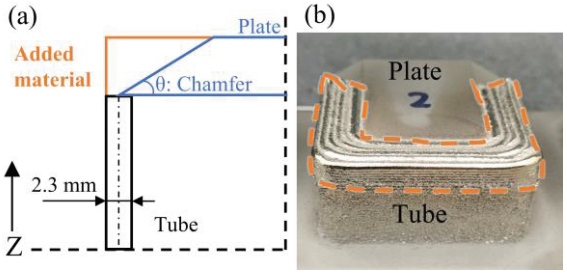

Figure 5: (a) Schematic representation of the overhang test and (b) welded 5 mm plate onto a tube by DED, highlighted with a dashed orange line.

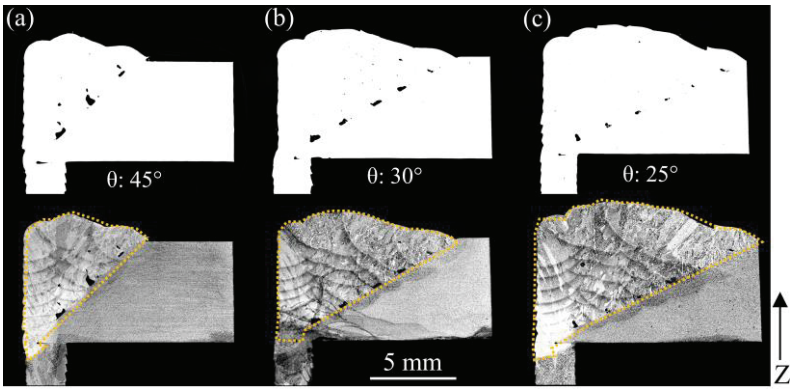

Figure 6: Polished (top) and etched (bottom) cross-sections of the overhang features where a horizontal plate is welded to a vertical tube with DED.

3.4 Production of the flaperon ribs

After the most characterising features were optimised, the manufacturing strategy of the flap ribs was defined. For that, the production of the ribs was divided into five operations (OP). The different operations are shown in Figure 7 depicted in different colours and showing the order of production by the numbering.

The first operation (OP1) consists of depositing the overthickness of the lugs and the thin-walled structure. The strategy followed for the overthickness was based on the deformation test results. The lugs were divided into 38 squares of 20x20 mm and rotated 60° with respect to the long axis of the substrate. Each square was deposited in a zig-zag manner, 90° rotated pattern between squares and built with an outside-in production order. In Figure 8(a), the first applied layer of this operation is shown. Together with the lug overthickness, the thin walls are built layer by layer. Due to the large deposited area and hence the high risk of deformation, symmetric deposition was carried out.

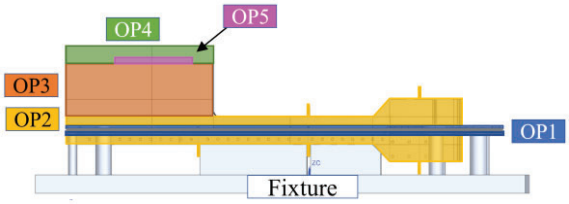

Figure 7: Schematic representation of the different operations (OP) and their production order.

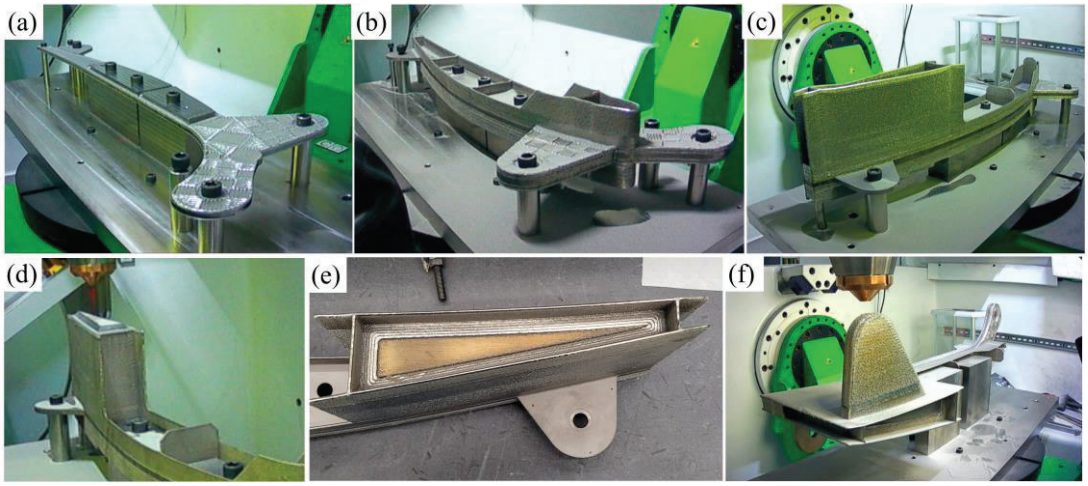

Figure 8: Picture of the rib during production, showing different steps of the process. (a-c) show the building of OP1-3, respectively. (d) and (e) show the welding of the horizontal web. In (f), OP5 is shown.

The second operation (OP2), involves the application of the thin-wall outer structure and the wall intersections. The contours and intersections were manufactured simultaneously and in a symmetric build-up manner. In Figure 8(b), a picture of this operation is shown.

After depositing all the symmetric features, in the third operation (OP3), the box structure was made. Since operation four (OP4) required a flat machined surface, 2 mm extra were built on top of the box. This operation is shown in Figure 8(c).

OP4 consists of welding the horizontal plate. For that, a plate was milled with 40° chamfers on all sides. Based on the pre-study, in order to ensure a good welding quality with DED, a smaller chamfer angle was preferred. However, the shape and the higher thickness of the plate (8 mm) did not allow machining a smaller chamfer angle.

In Figure 8(d) and (e), OP4 is shown where the overhang web is welded. After the box top surface was machined, the plate was placed and clamped in place. In order to ensure a good connection between the plate-box-deposition, 120% layer power was used for the first layer. After that, the welding of the plate was continued and the OP4 was finished. A picture of the finished welding operation is shown in Figure 8(e).

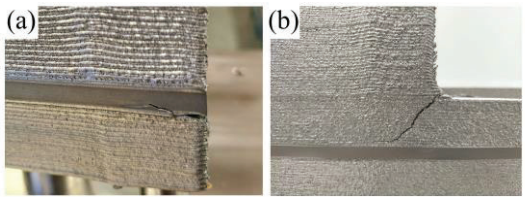

Figure 9: Examples of cracking and delamination that occurred during the production of the rib.

After following operations 1-4, the rib was stress relieved under vacuum while it was clamped in the fixture. This way the deformations were minimised, especially the remaining deformation in the substrate could be alleviated. It is advised to perform the stress relief treatment before machining since this step can cause cracking due to the vibrations, as shown in Figure 9.

The last operation (OP5) consists of building the overhanging lug on the side of the box structure. For that, the rib was rotated 90° along the long axis and fixed with a new clamping, as shown in Figure 8(f). Since the lug will be machined to size extra 3 mm were added. The first 20 mm were deposited by dividing the lug into two sections to mimic the checkerboard strategy. 45° vectors were chosen to avoid long vectors and hence, reduce the residual stresses. Between the island and layers, the pattern was rotated 45°. The upper part of the lug was manufactured only with one section and the same strategy was followed: 45° rotated vectors with 90° rotation between layers. The finished lug is shown in Figure 8(f).

After all operations were successfully carried out, the rib was again stress relieved. A picture of the finalised full-scale flaperon rib is shown in Figure 10. The total build duration where the machine was depositing was of 09:04 hours per rib. This time increases to 3 days considering the time within and between operations such as the time during symmetric deposition which consists of several flipping steps and cooling times in between.

Additive manufacturing of the full rib compared to conventional manufacturing is also interesting due to the improved BTF ratio. For producing a rib, 8.16 kg Ti6Al4V powder was used and the weight of the DED rib was 4.44 kg (of which 1.32 kg for the substrate and 0.24 kg for the web). This translates to a BTF ratio of less than 3:1 compared to the 40:1 ratio if the rib would be produced starting from a solid block.

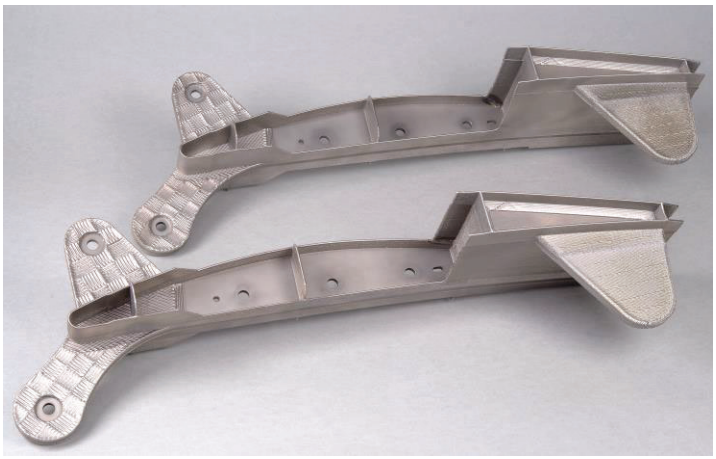

Figure 10: Finalised Ti6Al4V ribs for a flaperon assembly produced by powder DED.

4 Conclusions

- The optimum parameters for thin-walled features were selected for a thickness of 2.3 mm. The laser power, travel speed and wall intersection offset were optimised aiming at the lowest porosity.
- From the deformation tests, it was concluded that a symmetric build-up in combination with the island strategy leads to the least Z-deflection of the baseplate. It is advised to deposit material from outside to inside, in a zig-zag manner and to apply rotations between adjacent islands and layers.
- A horizontal overhanging web was successfully welded to a thin-walled structure using DED.
- Stress relieving treatments are necessary to reduce deformations, deformations and avoid cracking, in between critical steps and for the final product.
- Three full-scale flaperon ribs were successfully produced with a 3:1 BTF ratio and in a total of 3 days per rib.
- This work demonstrates the feasibility of producing complex and multi-functional aircraft components in titanium by laser powder DED.
- Further research should be performed on the mechanical performance of such complex components produced by DED.

Acknowledgements

This work was funded by the European Union's Horizon 2020 Clean Sky 2 research and innovation programme under grant agreement 945521 ITD/IADP/TA2, project MANTA.

Literature

[1] B. Blakey-Milner et al., "Metal additive manufacturing in aerospace: A review," Mater. Des., vol. 209, p. 110008, Nov. 2021, doi: 10.1016/j.matdes.2021.110008.

[2] J. Wang et al., "Effects of scanning strategies on residual stress and deformation by high-power direct energy deposition: Island size and laser jump strategy between islands," J. Manuf. Process., vol. 75, pp. 23–40, Mar. 2022, doi: 10.1016/j.jmapro.2021.12.054.

[3] M. Gebler, A. J. M. S. Uiterkamp, and C. Visser, "A global sustainability perspective on 3D printing technologies," Energy Policy, vol. 74, pp. 158–167, 2014, doi: https://doi.org/10.1016/j.enpol.2014.08.033.

[4] N. Shamsaei, A. Yadollahi, L. Bian, and S. M. Thompson, "An overview of Direct Laser Deposition for additive manufacturing; Part II: Mechanical behavior, process parameter optimization and control," Addit. Manuf., vol. 8, pp. 12–35, Oct. 2015, doi: 10.1016/j.addma.2015.07.002.

[5] Z. Liu, B. He, T. Lyu, and Y. Zou, "A Review on Additive Manufacturing of Titanium Alloys for Aerospace Applications: Directed Energy Deposition and Beyond Ti-6Al-4V," JOM, vol. 73, no. 6, pp. 1804–1818, Jun. 2021, doi: 10.1007/s11837-021-04670-6.

[6] D. Clark, M. T. Whittaker, and M. R. Bache, "Microstructural Characterization of a Prototype Titanium Alloy Structure Processed via Direct Laser Deposition (DLD)," Metall. Mater. Trans. B, vol. 43, pp. 388–396, 2011.

[7] A. Saboori, D. Gallo, S. Biamino, P. Fino, and M. Lombardi, "An Overview of Additive Manufacturing of Titanium Components by Directed Energy Deposition: Microstructure and Mechanical Properties," Appl. Sci., vol. 7, no. 9, 2017, doi: 10.3390/app7090883.

[8] ASTM International, "F3413-2019 Guide for Additive Manufacturing - Design - Directed Energy Deposition," 2019.